Journal of
Materials Chemistry A

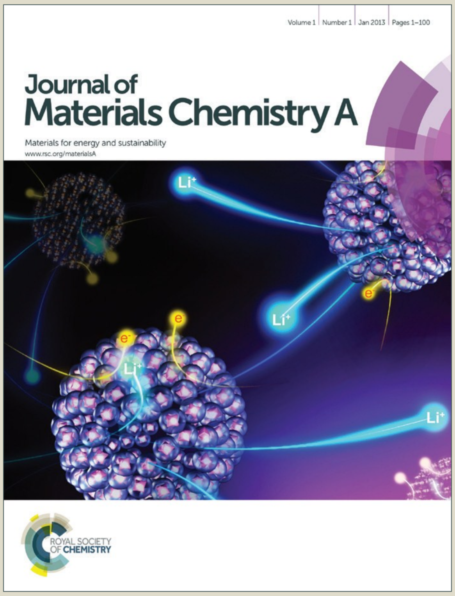

ROYAL SOCIETY
OF CHEMISTRY

www.rsc.org/materialsA

Journal Name

ARTICLE

High performance two-ply carbon nanocomposite yarn supercapacitors enhanced with platinum filament and in-situ polymerized polyaniline nanowires

Received 00th January 20xx,
Accepted 00th January 20xx

DOI: 10.1039/x0xx00000x

www.rsc.org/

Qiufan Wang,[a] Yunlong Wu,[a] Ting Li,[a] Daohong Zhang,[a*] Menghe Miao,[b*] Aiqing Zhang[a]

Two-ply yarn supercapacitors behave like conventional textile yarns to power next generation electronic textiles. To improve the capacitance of the yarn, we produced a metal filament reinforced carbon nanotube composite yarn which was further in-situ polymerized with polyaniline nanowires for use as electrodes. The wearable two-ply yarn supercapacitor made from the composite electrodes possesses very high capacitance (91.67 mF/cm^2) and energy density (12.68 μWh/cm^2), and excellent long term cycling stability for charging-discharging and flexing deformation. The two-ply nanocomposite yarn supercapacitors have been connected in series and in parallel to power miniature electronic devices on smart textiles.

Introduction

Because of their small size, light weight, and adaptability, flexible micro energy-storage devices are becoming an extremely attractive option for powering electronic textiles and portable electronics such as mobile phones, digital cameras, electronic tools, healthcare devices and rollup displays.[1-4] Flexible solid-state supercapacitors (SCs) offer much higher power density than conventional lithium ion batteries and much higher energy density than traditional capacitors.[5-10] In particular, linear SCs, or more technically known as two-ply yarn structured SCs, are highly flexible and can be integrated into fabrics like conventional textile yarns for use in next generation electronic textiles.[11-13]

Carbon nanotubes (CNTs) possess unique structures and outstanding mechanical and electrical properties. They have been studied extensively for applications in flexible electronics and energy storage.[14-15] CNTs can be spun into yarns.[16] Pure CNT yarn SCs are limited by their relatively low capacitance and energy density.[18] To improve the capacitance, high performance pseudocapacitance materials, such as metal oxide and conducting polymers, are incorporated into CNT yarn electrodes for use in flexible SCs.[19-21] Polyaniline has been proven to be a promising material for energy storage applications with its large capacitance and capability to charge and discharge at high rates.[22-23] Zhang et al. reported a core/sheath electrode architecture.[17a] in which CNTs form a thin surface layer around a highly conductive metal filament core. The metal filament serves as current collector so that charges produced on the active materials along the length of the SC are transported efficiently, resulting in a significant improvement in electrochemical performance and scale up of the SC length. The metal current collector can also be plied together with the CNT yarn by twisting.[17b] Here we report a high-performance wearable yarn SC that is formed from two composite yarns, each comprising of a platinum filament and a CNT yarn decorated with polyaniline nanowires by in-situ polymerization, dabbed as Pt/CNT@PANI composite yarn. The two-ply composite yarn SC deliveries very high energy density and cycling durability.

Experimental

Production of as-spun carbon nanotube yarns.

CNT forests were grown on silicon wafer substrates bearing a thermal oxide layer and iron catalyst coating using chemical vapour deposition (CVD) of acetylene in helium. The synthesis procedures have been reported previously.[24] The resulting CNTs had 7 ± 2 walls with an outer diameter of 10 nm and an inner diameter of 4 nm approximately. The length of the CNTs was approximately 350 μm by measuring the height of the forests. The CNT yarns were spun to a twist level of 5,000 turns/m using an Up-spinner.[16]

Preparation of Pt/CNT@PANI yarn.

0.18 g aniline and 0.4 mL ethanol were added into 200 mL $HClO_4$ (1 mmol/mL) aqueous solution, and then 0.304 g ammonium persulfate (24 mL) was added into the reaction solution at -10 ^{o} C. The Pt/CNT ply-yarn was placed in the above solution, after reacting for 24 h, the Pt/CNT yarn was removed and cleaned by ethanol and deionized water three times, respectively. The surface of Pt/CNT yarn became dark-green after the in-suit deposition.

Preparation of two-ply composite yarn supercapacitor.

PVA/H_3PO_4 gel electrolyte was prepared by mixing 3 g PVA and 3 g H_3PO_4 with 30 mL deionized water and heating it at 95 ^{o} C under

---

[a] Key Laboratory of Catalysis and Materials Science of the State Ethnic Affairs Commission & Ministry of Education, South-Central University for Nationalities, Wuhan, Hubei Province, 430074, China.
[b] CSIRO Manufacturing, 75 Pigdons Road, Waurn Ponds, Victoria 3216, Australia. E-mail: Menghe.Miao@csiro.au
* Dr. D.H. Zhang, Zhangdh27@163.com.
* Dr. M. H. Miao, E-mail: Menghe.Miao@csiro.au

Electronic Supplementary Information (ESI) available. See DOI: 10.1039/x0xx00000x vigorous stirring until it become clear. The Pt/CNT@PANI nanocomposite yarn were coated with PVA/H_3PO_4 three times and dried at 50 ^{o}C for 1 h. Two PVA/H_3PO_4 coated yarns were placed in parallel and twisted together, followed by coating with PVA/H_3PO_4 again to produce a solid-state two-ply nanocomposite yarn supercapacitor (SC)

Materials characterization.

Yarn morphology was characterized by scanning electron microscopy (SEM) and transmission electron microscopy (TEM). Cyclic voltammetry (CV), electrochemical impedance spectroscopy (EIS), and galvanostatic charge/discharge measurements were carried out on an electrochemical workstation (Ivium, CompactState10800).

Calculation of the electrochemical capacitance.

The as-prepared two-ply nanocomposite yarn SC is a symmetric two-electrode solid-state supercapacitor. The specific capacitance of SC obtained through cyclic voltammograms was based on the equation:

$$C = \frac{1}{\nu\, VS}\int_0^V I dV \qquad (1)$$

where C is the specific capacitance (F/cm^2), ν is the scan rate in cyclic voltammograms, *V* represents the potential window, and *I* stands for current. *S* is the surface area of the nanocomposite yarn in the overlap portion (cm^2).

The specific capacitance of SCs obtained through galvanostatic charge/discharge measurement was derived from the equation: $C_A = I\times t/(V\times S)$, where C_A is areal capacitance (F/cm^2), *I* stands for discharge current density (A), t is the discharge time (s), *V* represents the potential window (V), and *S* is the surface area of nanocomposite yarn in the overlap portion (cm^2). The area energy density (E_A) and areal power density (P_A) of the two-ply SC were obtained from $E_A = 1/2\times C_A\times V^2$ and $P_A = E_A/t$.

Results and discussion

A typical fabrication process of the two-ply nanocomposite yarn symmetric SCs based on carbon nanotube yarn and Pt filament is schematically shown in Figure 1. The substrate CNT yarn was fabricated by twisting a continuous CNT web drawn from a solid state multi-walled carbon nanotube forest which was synthesized using the chemical vapor deposition (CVD) method.[25-26] The yarn was spun to a twist density of 5000 turns/m. The Pt filament has good electrical conductivity and the CNT yarn has a porous structure. The combination of the Pt filament and the CNT yarn provides high electrolyte accessibility and high efficiency charge transport as well as the structural backbone of the two-ply composite yarn SC. The PANI nanowires polymerized in-situ on the surface of the twisted Pt/CNT yarn serves as the main electrochemically active material of the work electrode. The Pt/CNT@PANI nanocomposite yarn electrode is then coated with PVA/H3PO4 gel electrolyte. Two identical coated Pt/CNT@PANI nanocomposite yarn electrodes are combined together by twisting to form a two-ply nanocomposite yarn SC.

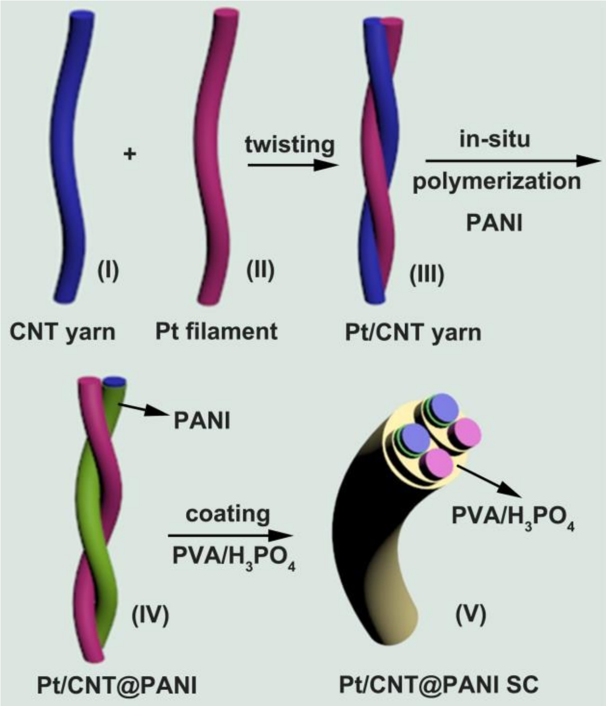

Figure 1. Schematic diagram of the fabrication process of the yarn SC.

The morphologies of the pure CNT yarn substrate and the final Pt/CNT@PANI nanocomposite yarn were examined using scanning electron microscopy (SEM) and transmission electron microscopy (TEM). Figure 2a shows the structure after the Pt filament and the CNT yarn being twisted together. Figure 2b and c exhibit SEM images of the as-spun pure CNT yarn at two magnifications, showing that the pure CNT yarn has porous microstructure and the CNTs are well aligned along the twist helix in the yarn. The yarn diameter is approximately 25 μm. The width of the twisted Pt/CNT yarn is approximately 50 μm. Figure 2d and e show the layer of PANI nanowires in-situ deposited on the surface of the twisted Pt/CNT yarn substrate. The PANI nanowires are uniform in diameter and form a porous layer on the CNT yarn surface. Figure S1 demonstrates that Pt wire did not attract any significant deposition of PANI nanowires. Figure 2f shows a TEM image of the PANI nanowires. The PANI nanowires have diameters about 40 nm and are tangled with each other, forming a porous network on the twisted Pt/CNT yarn surface. The chemical composition of the Pt/CNT@PANI composite yarn is further probed by Fourier transform infrared (FT-IR), and the results are shown in Figure 2f. The bands at 1569 and 1492 cm^{-1} are assigned to C=C stretching vibrations of quinoid and benzenoid rings, respectively. The bands at 1298, 1120, and 795 cm^{-1} originate from C-N, C=N, and C-H stretching vibration, respectively.[27-28] These results provide evidence that PANI has been successfully deposited on the CNT yarn.

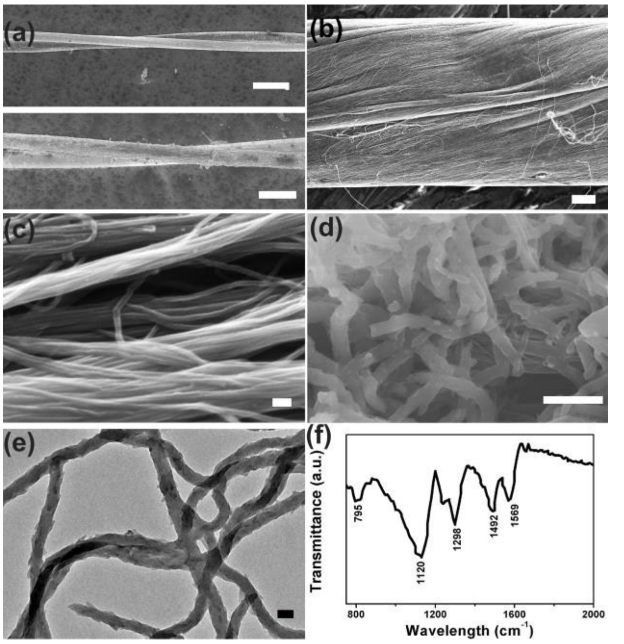

Figure 2. Electrode morphology. (a) twisted Pt/CNT yarn, (b-c) CNT yarn, (d) PANI nanowire network on Pt/CNT yarn, (e) TEM image of PANI nanowires and (f) FT-IR spectrum. Scale bars (from a to e): 100 µm, 4µm, 40 nm, 50 µm, 0.1 µm.

The electrochemical performances of the two-ply nanocomposite yarn SCs are tested in a two-electrode configuration. We first investigated the effect of PANI deposition time on the electrochemical performance of the Pt/CNT@PANI devices. Figure S2 and S3 in *Supporting Information* show the relationship between the electrode mass and device capacitance (500 mV/s) at different deposition durations. Prolonging deposition time from 17 h to 31 h increased the mass of PANI nanowire coating on the yarn due to gradual deposition of the PANI nanowires. However, the intermediate deposition duration (24 h) resulted in the highest capacitance, probably because of the increase of intrinsic resistance and the reduction of electrode conductivity associated with excessive growth time. The Figure S4 shows that 31 h polymerization time resulted in increased resistance.

Figure 3a shows the cyclic voltammograph (CV) curves at a wide range of scan rates from 10 mV/s to 500 mV/s of the Pt/CNT@PANI SC with an in-situ deposition time of 24 h. The CV curves show typical pseudocapacitive behaviours with two pairs of redox peaks, which are ascribed to the structural conversion of leucoemeraldine-to-emeraldine and emeraldine-to-pernigraniline of the PANI nanowires.[29-30]

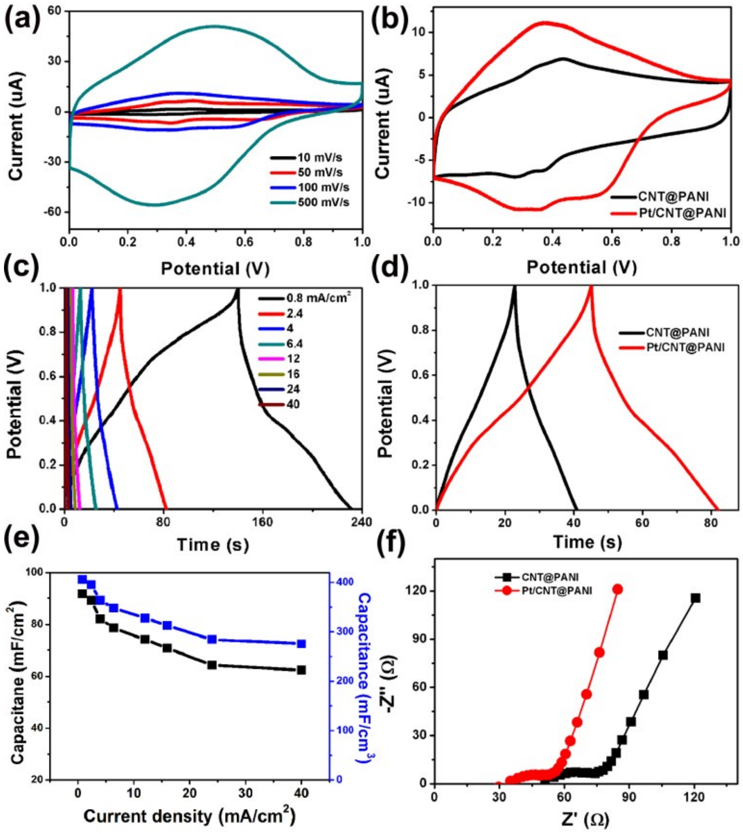

Figure 3. Electrochemical properties of two-ply nanocomposite yarn SCs: (a) cyclic voltammographs of Pt/CNT@PANI yarn SC, (b) CV curves of CNT@PANI and Pt/CNT@PANI yarn SCs at 100 mV/s, (c) galvanostatic charge/discharge curves of Pt/CNT@PANI yarn SC at different current densities, (d) charge/discharge curves for CNT@PANI and Pt/CNT@PANI SCs at 2.4 mA/cm^2, (e) areal capacitance of Pt/CNT@PANI yarn SC at different current densities, (f) impedance spectroscopy for CNT@PANI and Pt/CNT@PANI SC devices with a frequency loop from 100 KHz to 100 Hz using an amplitude of 5 mV at open-circuit potential.

At a high scan rate of 500 mV/s, the curves still have a symmetrical shape and show a 62% capacitance retention compared with a low scan rate of 10 mV/s. This indicates that the two-ply nanocomposite yarn SC has good capacitive performance and excellent rate capability. Figure S5 presents the CV curves of the Pt/CNT substrate and the final Pt/CNT@PANI nanocomposite yarn SCs at the scan rate of 100 mV/s. The CV curve of the Pt/CNT@PANI nanocomposite yarn SC shows a much larger surrounding area than the Pt/CNT substrate yarn SC, indicating dramatic improvement in capacitance attributable to the high pseudocapacitance of the PANI nanowire network.[31-34]

Figure 3b demonstrates the CV curves of the CNT@PANI and Pt/CNT@PANI yarn SCs at the scan rate of 100 mV/s. The Pt/CNT@PANI yarn SC demonstrates a considerably larger surrounding area of the CV curve, which can be attributed to the high conductivity of the Pt filament in the nanocomposite yarn as current collector. Figure 3c presents the galvanostatic charge/discharge curves of the Pt/CNT@PANI yarn SCs. The symmetrical profile of the charge and discharge curves indicates good capacitive performance of the solid-state device. The electrochemical performances of Pt/CNT and CNT@PANI SCs are provided in Figures S6 and S7 as comparisons. Figure 3d demonstrates the charge/discharge curves of the CNT@PANI and Pt/CNT@PANI nanocopmosite yarn SCs at the same current density of 2.4 mA/cm^2. Pt/CNT@PANI yarn SC demonstrates longer charge and discharge times than the CNT@PANI SC, indicating higher capacitance. This is consistent with the results from Figure 3b. The areal capacitance and capacitance retention of the Pt/CNT@PANI nanocopmosite yarn SC at different discharge current densities is plotted in Figure 3e. At 0.8 mA/cm^2, the areal capacitance reached *ca*. 97.67 mF/cm^2 (405.5 mF/cm^3). This value is about 27-fold of the reported value for rGO/CNT yarn SC (3.3 mF/cm^2 at 0.8 mA/cm^2),[35] 7 times as much as that for the SC based on CNT@PANI yarn (13 mF/cm^2 at 0.8 mA/cm^2),[36] or 5 times as much as that of the CNT@Co$_3$O$_4$ yarn SC (18 mF/cm^2).[37] This capacitance is also much greater than those of flexible linear-SCs based on CNT@PEDOT.[38] When the current density was increased by 50 times from 0.8 to 40 mA/cm^2, the capacitance maintains at 68% of its initial level, demonstrating good stability over a very wide range of current density. Figure S8 further exhibits the performances of the devices fabricated using shorter and longer (17 h and 31 h) durations of PANI nanowire deposition, respectively.

Electrochemical impedance spectroscopy (EIS) is used to investigate the complex impedance and ion diffusion process of the SCs in the frequency ranging from 100 Hz to 100 KHz. The intercept of the Nyquist impedance plot with X-axis and the diameter of the semicircle in the high frequency region represent respectively the equivalent series resistance (ESR) and the interfacial charge transfer resistance.[39a] As shown in Figure 3f, the Pt/CNT@PANI-based supercapacitor exhibits lower ESR, which can be ascribed to the improved conductivity of the Pt/CNT@PANI nanocomposite yarn electrode. This architecture also facilitates the efficient access of electrolyte ions to the CNT and shortens the ion diffusion distance. The diameter of the Pt/CNT@PANI-based supercapacitor is smaller (30 ohm) than CNT@PANI-based supercapacitor (42 ohm), demonstrating a smaller charge transfer resistance. The slope of the Nyquist plots, often referred to Warburg resistance. The slope of the straight line in the middle-frequency region of the two yarn supercapacitors is larger than 45^o, indicating typical capacitor behavior. The Pt/CNT@PANI-based supercapacitor display shorter Warburg curves, which is evidence of shorter ion diffusion path.[41]

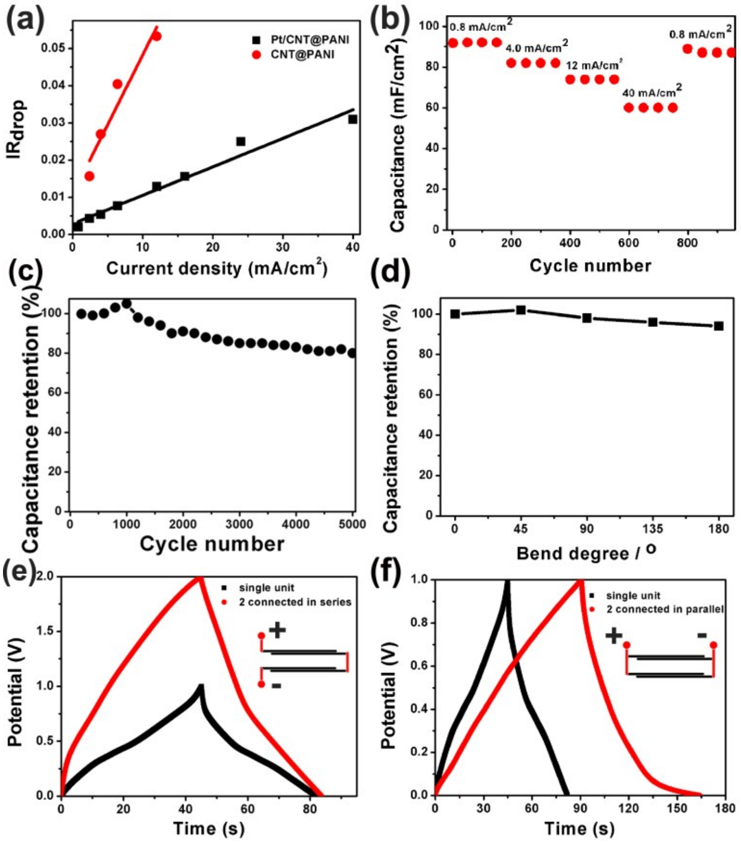

Figure 4. Further characterization of the Pt/CNT@PANI nanocomposite yarn supercapacitor. (a) drop of cell internal resistance (IR loss) as a function of discharge current density, (b) cycle performance at varying current density, (c) capacitance retention at different charging/discharging cycles at constant current density 4 mA/cm^2, (d) capacitance retention under different bending states, (e) galvanostatic charge/discharge of two devices connected in series, (f) galvanostatic charge/discharge of two devices connected in parallel.

The IR drop that is estimated at the beginning of the discharge curve[39b] of the CNT@PANI and Pt/CNT@PANI yarn SCs are plotted against the current density in Figure 4a. Obviously, the Pt/CNT@PANI yarn SC shows much smaller IR drop and a less steep slope than the CNT@PANI yarn SC, which is consistent with Figure 3f. The cyclic performance of the Pt/CNT@PANI yarn SC at progressively increased current density is shown in Figure 4b. The continuous cycling was carried out first at the current density of 0.8 mA/cm^2 for 200 cycles, then at gradually increasing current densities of 4.0, 12.0 and 40.0 mA/cm^2 for 200 cycles at each subsequent step, and finally back to 0.8 mA/cm^2 to complete a total of 1000 cycles. The final capacitance at 0.8 mA/cm^2 was as much as 87% of the initial capacitance before the cycling test. The long-term cycling performance of the Pt/CNT@PANI yarn SC was tested for 5000 cycles at the current density of 4 mA/cm^2. The device exhibited 80% retention of its initial capacitance. This excellent stability can be attributed to the good contact between the individual CNTs and the PANI nanowires in the nanocomposite yarn and the excellent conductivity of the twisted Pt/CNT yarn substrate as current collector. The Pt/CNT@PANI nanocomposite yarn SC is very flexible and a 1 cm long SC specimen can be bent to any degree with negligible loss of capacitance (Figure 4d).

In commercial applications of SCs, it is often necessary to connect SC in series and/or in parallel to increase the operating voltage and capacitance. Figure 4e shows the charge/discharge curves of a single unit and a pack of two units connected in series tested at the same current density 2.4 mA/cm^2. The calculated capacitances of the electrochemical capacitor series pack was 58.45 μF, or a half of that of the single unit (107.87 μF), and the operating potential window was increased to 2 V. Figure 4f exhibits the charge/discharge curves of a single SC and two SCs connected in parallel tested at the same current density 2.4 mA/cm^2. The total capacitance of the parallel system was 220.6 μF, twice of the capacitance of a single SC. The results show that the two-ply nanocomposite yarn device obeys the laws for capacitors in series and in parallel. Therefore the as-fabricated yarn SCs can be connected in series or in parallel to meet specific voltage and capacitance requirements for any given application.

Energy density and power density are two important parameters used to evaluate performance of energy storage devices. Figure 5 presents the Ragone plot of the Pt/CNT@PANI nanocomposite yarn SC calculated from galvanostatic discharge curves. The areal energy density of the device varies from 12.68 to 8.13 μWh/cm^2 with corresponding power densities from 399 to 19381 μW/cm^2. The energy density in this work is very high when compared to other recently reported two-ply yarn SCs, for example, OMC/CNT yarn (1.77 μWh/cm^2 at 32 μW/cm^2),[35] RGO+CNT@CMC yarn (3.84 μWh/cm^2 20 μW/cm^2),[3] CNT@Co_3O_4 yarn SC (1.1 μWh/cm^2 10 uW/cm^2)[37] and CNT/ordered mescoporous carbon (1.77 μWh/cm^2 17 μW/cm^2).[40] The high energy density can be ascribed to the PANI nanowire network on the CNT yarn surface that offers a large efficient specific area for ion absorption in the electrolyte and the high charge transport efficiency of the metal filament incorporated in the electrode. The inset picture in Figure 5 shows that two micro-sized SCs in series can power a small electronic device, such as a LED indicator, showing huge prospects for electronic textiles.

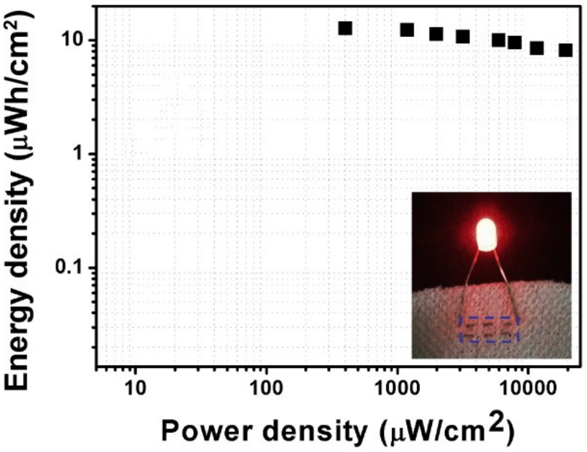

Figure 5. Ragone plots of the linear device fabricated according to the method in this paper in comparison with recently reported linear devices. Inset picture shows that a LED indicator powered by two Pt/CNT@PANI nanocomposite yarn SCs connected in series.

Conclusions

An all-solid-state, highly flexible two-ply yarn supercapacitor based on Pt/CNT@PANI nanowire nanocomposite material has been successfully designed and fabricated. The device has demonstrated excellent flexibility and performance, including high capacitance (91.67 mF/cm^2), energy density (12.68 μWh/cm^2) and excellent cycling stability (80% capacitance retention after 5000 cycles). A number of such two-ply nanocomposite yarn supercapacitors can be connected in series and in parallel to form a supercapacitor fabric for powering portable and wearable electronic devices.

Acknowledgements

We gratefully acknowledge the financial support of Hubei Province Natural Science Fund for Distinguished Young Scientists (2014CFA037) and the Program for New Century-Talents in Universities (NCET-13-1049).

Notes and references

‡ Footnotes relating to the main text should appear here. These might include comments relevant to but not central to the matter under discussion, limited experimental and spectral data, and crystallographic data.

1 M. F. El-Kady, V. Strong, S. Dubin, R. B. Kaner, *Science*, 2012, 335, 1326.
2 M. Kaempgen, C. K. Chan , J. Ma , Y. Cui , G. Gruner, *Nano Lett*., 2009, 9, 1872.
3 L. Kou, T. Huang, B. Zheng, Y. Han, X. Zhao, K. Gopalsamy, H. Sun, C. Gao, *Nat. Commun.*, 2014, 5, 3754.

4 H. X. Zhang , C. Feng , Y. C. Zhai , K. L. Jiang , Q. Q. Li , S. S. Fan, *Adv. Mater.*, 2009, 21, 2299.

5 P. Simon, Y. Gogotsi, *Nat. Mater*., 2008, 7, 845.

6 J. R. Miller, P. Simon, *Science*, 2008, 321, 651.

7 C. Zhou, Y. W. Zhang, Y. Y. Li, J. P. Liu, *Nano Lett*., 2013, 13, 2078.

8 M. F. El-Kady, V. Strong, S. Dubin, R. B. Kaner, *Science*, 2012, 335, 1326.

9 Y. Xu, Z. Lin, X. Huang, Y. Liu, Y. Huang, X. Duan, *ACS Nano*, 2013, 7, 4042.

10 X. Xiao, T. Q. Li, P. H. Yang, Y. Gao, H. Y. Jin, W. J. Ni, W. H. Zhan, X. H. Zhang, Y. Z. Cao, J. W. Zhong, L. Gong ,W.-C. Yen, W. J. Mai, J. Chen, K. F. Huo, Y.-L. Chueh, Z. L. Wang, J. Zhou, *ACS Nano*, 2012, 6, 9200.

11 K. Wang, H. P. Wu, Y. N. Meng, Z. X. Wei, *Small*, 2014, 10, 14.

12 S. H. Aboutalebi, R. Jalili, D. Esrafilzadeh, M. Salari, Z. Gholamvand, S. Aminorroaya Yamini, K. Konstantinov, R. Shepherd, J. Chen, S. Moulton, P. C. Innis, A. Minett, J. Razal, G. Wallace, *ACS Nano*, 2014, 8, 2456.

13 C. Choi, J. A. Lee, A. Y. Choi, Y. T. Kim, X. Lepro, M. Lima, R. Baughman, S. J. Kim, *Adv. Mater.*, 2014, 26, 2059.

14 K. L. Jiang, J. P. Wang, Q. Q. Li, L. Liu, C. H. Liu, S. S. Fan, *Adv. Mater.*, 2011, 23, 1154.

15 K. Liu, Y. H. Sun, R. F. Zhou, H. Y. Zhu, J. P. Wang, L. Liu, S. S. Fan, K. L. Jiang, *Nanotechnology*, 2010, 21, 04570.

16 M. H. Miao, *Particuology*, 2013, 11, 378-393.

17 a) D. H. Zhang, M. H. Miao, H. T. Niu, Z. X. Wei, *ACS Nano*, 2014, 8, 4571; b) D. H. Zhang, Y. L. Wu. T. Li, Y. Huang, A. Q. Zhang, M. H. Miao, *ACS Appl. Mater. Interfaces*, 2015, DOI: 10. 1020/acsami.5b08110.

18 T. Mirfakhrai, J. Oh, M. Kozlov, E. Fok, M. Zhang, S. Fang, R. Baughman, J. Madden, *Smart. Mater. Struct*., 2007, 16, S24.

19 G. P. Wang, L. Zhang, J. J. Zhang, *Chem. Soc. Rev*., 2012, 41, 797.

20 J. H. Zhong, A.L. Wang, G.R. Li, J.W. Wang, Y.N. Ou, Y.X. Tong, *J. Mater. Chem.*, 2012, 22, 5656.

21 Z. Chen, V. Augustyn, J. Wen, Y. W. Zhang, M. Q. Shen, B. Dunn, Y. F. Lu, *Adv. Mater.*, 2011, 23, 791.

22 Z. G. Yin, Q. D. Zheng, *Adv. Energy Mater.*, 2012, 2, 179.

23 S. I1 Cho, S. B. Lee, *Acc. Chem. Res.*, 2008, 41, 699.

24 C. P. Huynh, S. C. Hawkins, *Carbon*, 2010, 48, 1105.

25 M. H. Miao, S. C. Hawkins, J. Y. Cai, T. R. Gengenbach, R. Knott, C. P. Huynh, *Carbon*, 2011, 49, 4940.

26 M. H. Miao, *Carbon*, 2011, 49, 3755.

27 L. Y. Yuan, X. Xiao, T. Ding, J. Zhong, X. Zhang, Y. Shen, B. Hu, Y. Huang, J. Zhou, Z. L. Wang, *Angew. Chem., Int. Ed.*, 2012, 51, 4931.

28 X. Zeng, T. Ko, *Polym. Sci*., 1997, 35, 1993.

29 W. Feng, Q. Zhang, Y. Li, Y. Feng, *J. Solid State Electrochem.*, 2013, 18, 1127.

30 P. P. Yu, X. Zhao, Z. L. Huang, Y. Li, Q. H. Zhang, *J. Mater. Chem. A*, 2014, 2, 14413.

31 K. Wang, W. J. Zou, B. G. Quan, A. F. Yu, H. P. Wu, P. Jiang, Z. X. Wei, *Adv. Energy Mater*., 2011, 1, 1068.

32 K. Wang, P. Zhao, X. M. Zhou, H. P. Wu, Z. X. Wei, *J. Mater. Chem.*, 2011, 21, 16373.

33 K. Wang, H. P. Wu, Y. N. Meng, Y. J. Zhang, Z. X. Wei, *Energy Environ. Sci*., 2012, 5, 8384.

34 K. Wang , J. Y. Huang , Z. X. Wei, *J. Phys. Chem. C*, 2010, 114, 8062.

35 J. Ren, L. Li, C. Chen, X. L. Chen, Z. B. Cai, L. B. Qiu, Y. G. Wang, X. R. Zhu, H. S. Peng, *Adv. Mater.*, 2013, 25, 1155.

36 K. Wang, Q. H. Meng, Y. J. Zhang, Z. X. Wei, M. H. Miao, *Adv. Mater.*, 2013, 25, 1494.

37 F. H. Su, X. M. Lv, M. H. Miao, *Small*, 2015, 7, 854.

38 J. A. Lee, M. K. Shin, S. H. Kim, H. U. Cho, G. M. Spinks, G. G. Wallace, M. D. Lima, X. Lepro, M. E. Kozlov, R. H. Baughman, S. J. Kim, S. Kim, *Nat. Commun.*, 2013, 4, 1970.

39 a) A. T. Chidembo, S. H. Aboutalebi, K. Konstantinov, D. Wexler, H. K. Liu, S. X. Dou, *Part. Part. Syst. Charact.*, 2014, 31, 465; b) J. Xu, Q. F. Wang, X. W. Wang, Q. Y. Xiang, B. Liang, D. Chen, G. Z. Shen, *ACS Nano*, 2013, 7, 5453.

40 J. Ren, W. Y. Bai, G. Z. Guan, Y. Zhang, H. S. Peng, *Adv. Mater.*, 2013, 25, 5965.

41 L. Zhang, G. Shi, *J. Phys. Chem. C*, 2011, 115, 17206-17212.

Two-ply yarn supercapacitor fabricated from Pt/CNT@PANI nanowire composite electrodes exhibits high specific capacitance 91.67 mF/cm^2 and high energy density 12.68 μWh/cm^2. A number of such linear supercapacitors can be connected together to power wearable electronic devices.

High performance wearable two-ply carbon nanocomposite yarn supercapacitors enhanced with platinum filament and in-situ polymerized polyaniline nanowires